

Probing the Specificity of the Serine Proteases Subtilisin Carlsberg and α -Chymotrypsin with Enantiomeric 1-Acetamido Boronic Acids. An Unexpected Reversal of the Normal “L”-Stereoselectivity Preference

Valeri Martichonok and J. Bryan Jones*

Contribution from the Lash Miller Laboratories, Department of Chemistry, University of Toronto, 80 St. George Street, Toronto, Canada M5S 1A1

Received August 15, 1995[®]

Abstract: Enantiomeric 1-acetamido boronic acids, which are *N*-acetyl transition state analog inhibitor analogs of L- and D-forms of the amino acids alanine, phenylalanine, *p*-fluorophenylalanine, *p*-chlorophenylalanine, and 1-naphthylalanine, have been evaluated as inhibitors of the serine proteases subtilisin Carlsberg (SC) and α -chymotrypsin (CT). All of the boronic acids are powerful competitive inhibitors of both enzymes, with, as expected, the L-enantiomers being generally more potent than the D-enantiomers. However, a dramatic reversal of the normal stereoselectivity preference was observed in the inhibition of CT by [1-acetamido-2-(1-naphthyl)ethyl]boronic acid, with the D-enantiomer becoming a 25-fold more potent inhibitor than the L-enantiomer. Furthermore, the K_i of 127 nM for CT inhibition by this D-enantiomer is the lowest of any of the boronic acids evaluated. Molecular modeling analyses of the possible binding modes of the inhibitors suggest that the stereoselectivity reversal is due to S_1 -pocket orientations of naphthyl groups that are different from those of the aromatic side chains of the phenylalanine analogs.

Enzymes are now widely used in synthetic organic chemistry, with their abilities to be highly stereoselective in their catalyses being extensively exploited in asymmetric synthesis.¹ However, the factors responsible for determining the structural and stereospecificity of enzymes toward unnatural substrates and inhibitors remain poorly understood. We became interested in this area² because, in order to identify the enzymes best suited to coping with the increasingly broad chiral synthon demands of asymmetric synthesis, it is important that the factors controlling substrate binding and orientation be identified.

With synthetic applications of hydrolytic enzymes being of such widespread current interest,¹ the serine proteases subtilisin Carlsberg (SC; EC 3.4.21.14) and α -chymotrypsin (CT; EC 3.4.21.1) were selected as representative esterases for stereospecificity studies. SC and CT are commercially available enzymes that have been extensively applied synthetically³ and for which high-resolution X-ray crystal structures are avail-

able.^{4,5} In both SC and CT, the active site binding regions are composed of several subsites, of which the S_1 ⁶-pocket dominates, particularly in the binding of hydrophobic groups. While in their catalyses of hydrolyses of their natural protein substrates, and of related amino acid esters, both enzymes exhibit a dominant stereoselectivity preference for the L-amino acid configuration, forecasting their stereoselectivities for unnatural substrates is not straightforward. Even for amino acid esters, reversals of stereoselectivity, *i.e.*, to prefer D over L,^{7,8} can be induced within a homologous series.⁹ Furthermore, the substrate specificity of SC and CT can be modified when water is replaced with a nonaqueous solvent,¹⁰ and some inversion of enzyme enantioselectivity can be induced by switching solvents.¹¹ Also, in supercritical fluids the degree of enantioselectivity can be tuned by changing the pressure.¹²

[®] Abstract published in *Advance ACS Abstracts*, January 1, 1996.

(1) (a) *Enzymes in Synthetic Organic Chemistry*; Wong, C.-H., Whitesides, G. M., Eds.; Pergamon: New York, 1994. (b) *Preparative Biotransformations*; Roberts, S. M., Ed.; Wiley: New York, 1993. (c) *Biotransformations in Preparative Organic Chemistry*; Faber, K., Ed.; Springer-Verlag: Heidelberg, 1992.

(2) (a) Jones, J. B. *Aldrichim. Acta* **1993**, 26, 105. (b) Bonneau, P. R.; Eyer, M.; Graycar, T. P.; Estell, D. A.; Jones, J. B. *Bioorg. Chem.* **1993**, 21, 431. (c) Jones, J. B. *Can. J. Chem.* **1993**, 71, 1273. (d) Bonneau, P. R.; Graycar, T. P.; Estell, D. A.; Jones, J. B. *J. Am. Chem. Soc.* **1991**, 113, 1026. (e) Lee, T.; Jones, J. B. *Tetrahedron* **1995**, 51, 7331.

(3) (a) Delinck, D. L.; Margolin, A. L. *Tetrahedron Lett.* **1990**, 31, 3093. (b) Pugniere, M.; San Juan, C.; Previero, A. *Tetrahedron Lett.* **1990**, 31, 4883. (c) Gotor, V.; Garcia, M. J.; Rebelleo, F. *Tetrahedron: Asymmetry* **1990**, 1, 277. (d) Margolin, A. L.; Delinck, D. L.; Whalon, M. R. *J. Am. Chem. Soc.* **1990**, 112, 2849. (e) Chenevert, R.; Desjardins, M.; Gagnon, R. *Chem. Lett.* **1990**, 33. (f) Chenevert, R.; Letourneau, M.; Thiboutot, S. *Can. J. Chem.* **1990**, 960. (h) Frigerio, F.; Coda, A.; Pugliese, L.; Lionetti, C.; Menegatti, E.; Amiconi, G.; Schnebli, H. P.; Ascenzi, P.; Bolognesi, M. *J. Mol. Biol.* **1992**, 225, 107. (i) Ricca, J. M.; Crout, D. H. *J. Chem. Soc., Perkin Trans. 1* **1989**, 2126. (j) Kitaguchi, H.; Fitzpatrick, P. A.; Huber, J. E.; Klibanov, A. M. *J. Am. Chem. Soc.* **1989**, 111, 3094. (k) Brieve, R.; Rebelleo, F.; Gotor, V. *J. Chem. Soc., Chem. Commun.* **1990**, 1386. (l) Gutman, A. L.; Meyer, E.; Kalerin, E.; Polyak, F.; Sterling, J. *Biotechnol. Bioeng.* **1992**, 40, 760. (m) Roper, J. M.; Bauer, D. P. *Synthesis* **1983**, 1041.

(4) (a) McPhalen, C. A.; James, M. N. G. *Biochemistry* **1988**, 27, 6582. (b) Bode, W.; Papamokos, E.; Musil, D. *Eur. J. Biochem.* **1987**, 166, 673.

(5) (a) Frigerio, F.; Coda, A.; Pugliese, L.; Lionetti, C.; Menegatti, E.; Amiconi, G.; Schnebli, H. P.; Ascenzi, P.; Bolognesi, M. *J. Mol. Biol.* **1992**, 225, 107. (b) Tsukada, H.; Blow, D. M. *J. Mol. Biol.* **1985**, 184, 703. (c) Birktoft, J. J.; Blow, D. M. *J. Mol. Biol.* **1972**, 68, 187. (d) Blevins, R. A.; Tulinsky, A. *J. Biol. Chem.* **1985**, 260, 4264. (e) Tulinsky, A.; Blevins, R. A. *J. Biol. Chem.* **1987**, 262, 7737.

(6) (a) Schechter, I.; Berger, A. *Biochem. Biophys. Res. Commun.* **1967**, 27, 157. (b) Berger, A.; Schechter, I. *Philos. Trans. R. Soc. London, Ser. B* **1970**, 257, 249.

(7) It should be noted that for the first apparent example of a CT preference of a D- over an L-substrate,⁸ the D-center is actually of the L-amino acid configuration type.

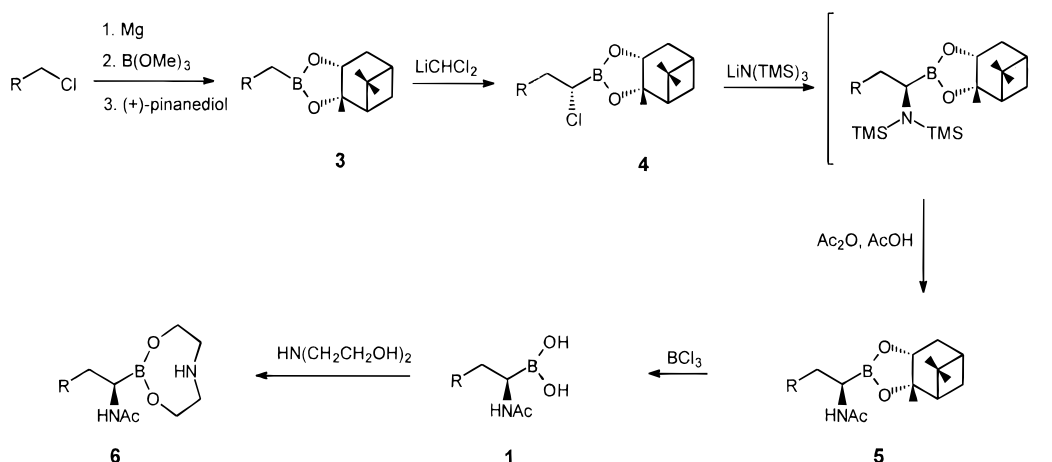
(8) Hein, G. E.; McGriff, R. B.; Niemann, C. *J. Am. Chem. Soc.* **1960**, 82, 1830. Hein, G. E.; Niemann, C. *J. Am. Chem. Soc.*, **1962**, 84, 4487. (See also: Jones, J. B., Beck, J. F. *Tech. Chem. (N. Y.)*, **1976**, 10, 172–185).

(9) Schwartz, H. M.; Wu, W. -S.; Marr, P. W. Jones, J. B. *J. Am. Chem. Soc.* **1978**, 100, 5199.

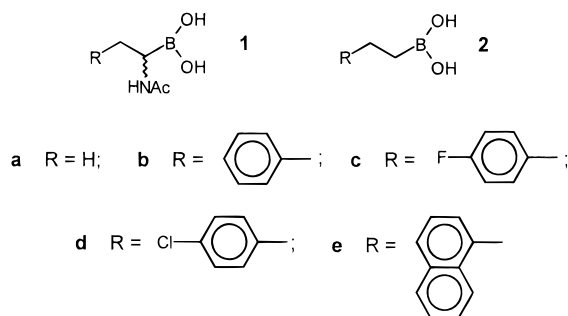
(10) Wescott, C. R.; Klibanov, A. M. *J. Am. Chem. Soc.* **1993**, 115, 1629.

(11) (a) Tawaki, S.; Klibanov, A. M. *J. Am. Chem. Soc.* **1992**, 114, 1882. (b) Orsat, B.; Drtina, G. J.; Williams, M. G.; Klibanov, A. *Biotechnol. Bioeng.* **1994**, 44, 1265. (c) Wescott, C. R.; Klibanov, A. M. *Biochim. Biophys. Acta* **1994**, 1206, 1. (d) Wescott, C. R.; Klibanov, A. M. *J. Am. Chem. Soc.* **1993**, 115, 10362. (e) Yennawar, H. P.; Yennawar, N. H.; Farber, G. K. *J. Am. Chem. Soc.* **1995**, 117, 577.

Scheme 1



In our previous probing of enzyme specificity,¹³ the strategy of evaluating the binding affinities of boronic acid transition state analog competitive inhibitors¹⁴ was followed, coupled with graphics analyses and molecular modeling. Boronic acids are generally very effective, reversible, transition state inhibitors of serine proteases^{14,15} and have proved well suited for the systematic probing of the structural and electrostatic specificity of the S₁-site of SC for achiral boronic acid inhibitors.¹³ Accordingly, the same strategy has been adopted for probing stereoselectivity determinants, using enantiomeric 1-acetamido boronic acids **1a–e**, whose structures mimic known *N*-acetyl-amino acid ester substrates, as transition state analog inhibitors of SC and CT. Both L- and D-enantiomers were included since, while *N*-acetyl-D-amino acid esters are not serine protease substrates, they are able to bind at the same active site locations as their L-substrate counterparts and can be effective competitive inhibitors.¹⁶ The achiral parent boronic acids **2a–e** were also included for reference purposes.



Results and Discussion

Preparation of Boronic Acids. The L-(*R*)- and D-(*S*)-1-acetamido boronic acids used for this study were prepared, as shown in Scheme 1 for the L-(*R*)-series, employing the basic strategy developed by Matteson et al.^{15h,17} Matteson homologation¹⁸ of the pinanediol esters **3a–e** gave the α -chloro boronic esters **4a–e** in 75–95% yields with diastereoselectivities >98%. Treatment of the α -chloro boronic esters **4** with lithium

hexamethyldisilazane afforded the corresponding silylated amino boronic esters, which were unstable and were treated directly with acetic acid and acetic anhydride at -78°C according to the Matteson protocol.¹⁹ The formation of the 1-acetamido boronic esters **5a–e** occurred with complete inversion. Pinanediol esters are very resistant to the hydrolysis, and the **5** \rightarrow **1** conversions required cleavage with boron trichloride at -78°C . Boronic acids are notoriously difficult to characterize in terms of elemental composition because of the ease with which they fully or partially dehydrate to the corresponding trimeric, or oligomeric in the case of **1a**, anhydrides. Accordingly, all of the target inhibitors L- and D-**1a–e** were further characterized as their stable, crystalline, diethanolamine derivatives **6** by reaction with diethanolamine in 2-propanol.^{18b,d} This derivatization also provided protection against possible autoxidation²⁰ of the acetamido boronic acids **1** by atmospheric oxygen. Both the anhydride forms of **1** and the diethanolamine derivatives **6** are immediately and quantitatively hydrolyzed to the corresponding free boronic acids on solution in water.

(12) (Kamat, S. V.; Beckman, E. J.; Russell, A. J. *J. Am. Chem. Soc.* **1993**, *115*, 8845.

(13) (a) Keller, T. H.; Seuffer-Wasserthal, P.; Jones, J. B. *Biochem. Biophys. Res. Commun.* **1991**, *176*, 401. (b) Seuffer-Wasserthal, P.; Martichonok, V.; Keller, T. H.; Chin, B.; Martin, R.; Jones, J. B. *Bioorg. Med. Chem.* **1994**, *2*, 35.

(14) (a) Koehler, K. A.; Lienhard, G. E. *Biochemistry* **1971**, *10*, 2477. (b) Raw, J. D.; Lienhard, G. E. *Biochemistry* **1974**, *13*, 3124. (c) Phillip, M.; Bender, M. L. *Proc. Natl. Acad. Sci. U.S.A.* **1971**, *68*, 478. (d) Antonov, V. K.; Ivanina, T. V.; Berezin, I. V.; Martinek, K. *FEBS Lett.* **1970**, *7*, 23. (e) Wolfenden, R. *Acc. Chem. Res.* **1972**, *5*, 10.

(15) (a) Westmark, P. R.; Kelly, J. P.; Smith, B. R. *J. Am. Chem. Soc.* **1993**, *115*, 3416. Baldwin, J. E.; Smith, B. D.; Claridge, T.; Derome, A.; Schofield, C. J. *Bioorg. Med. Chem. Lett.* **1991**, *1*, 9. (b) Elgandy, S.; Deadman, J.; Patel, G.; Green, D.; Chino, N.; Goodwin, C. A.; Scully, M. F.; Kakkar, V. V.; Claeson, G. *Tetrahedron Lett.* **1992**, *33*, 4209. (c) Kettner, C.; Mersinger, L.; Knaubb, R. *J. Biol. Chem.* **1990**, *265*, 18289. (d) Abouakil, N.; Lombardo, D. *Biochim. Biophys. Acta* **1989**, *1004*, 215. (e) Crompton, I. E.; Cuthbert, B. K.; Lowe, C.; Waley, S. G. *Biochem. J.* **1988**, *251*, 453. (f) Goz, B.; Ganguli, C.; Troconis, M.; Wyrick, S.; Isahq, K. S.; Katzenellenbogen, J. A. *Biochem. Pharmacol.* **1986**, *35*, 3587. (g) Kinder, D. H.; Katzenellenbogen, J. A. *J. Med. Chem.* **1985**, *28*, 1917. (h) Kettner, C. A.; Shenvi, A. B. *J. Biol. Chem.* **1984**, *259*, 15106. (i) Tsai, I. H.; Bender, M. L. *Arch. Biochem. Biophys.* **1984**, *228*, 555. (j) Matteson, D. S.; Sadhu, K. M.; Lienhard, G. F. *J. Am. Chem. Soc.* **1981**, *103*, 5241. (k) Garner, C. W. *J. Biol. Chem.* **1980**, *255*, 5064. (l) Nakatani, H.; Uehara, Y.; Hiromi, K. *J. Biochem.* **1975**, *78*, 611.

(16) (a) Foster, R. J.; Niemann, C. *J. Am. Chem. Soc.* **1955**, *77*, 1886. (b) Foster, R. J.; Shine, H. J.; Niemann, C. *J. Am. Chem. Soc.* **1955**, *77*, 2378. (c) Manning, D. T.; Niemann, C. *J. Am. Chem. Soc.* **1958**, *80*, 1478.

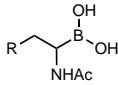
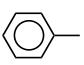
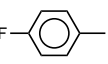
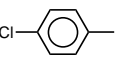
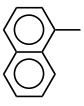
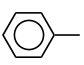
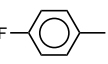
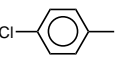
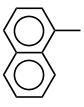
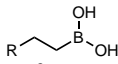
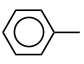
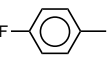
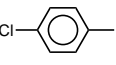
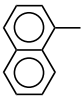
(17) (a) Matteson, D. S.; Sadhu, K. M. *Organometallics* **1984**, *3*, 614. (b) Matteson, D. S.; Michnick, T. J.; Willett, R. D.; Patterson, C. D. *Organometallics* **1989**, *8*, 726. (c) Matteson, D. S.; Michnick, T. J. *J. Labelled Compd. Radiopharm.* **1992**, *31*, 567.

(18) (a) Matteson, D. S.; Majumdar, D. *Organometallics* **1983**, *2*, 1529. (b) Tripathy, P. B.; Matteson, D. S. *Synthesis* **1990**, 200. (c) Matteson, D. S.; Sadhu, K. M.; Peterson, M. L. *J. Am. Chem. Soc.* **1986**, *108*, 810. (d) Matteson, D. S.; Ray, R.; Rocks, R. R.; Tsai, D. J. S. *Organometallics* **1983**, *2*, 1536. (e) Matteson, D. S.; Majumdar, D. *J. Am. Chem. Soc.* **1980**, *102*, 7588. (f) Matteson, D. S.; Ray, R. *J. Am. Chem. Soc.* **1980**, *102*, 7590. (g) Matteson, D. S.; Erdik, E. *Organometallics* **1983**, *2*, 1083. (h) Matteson, D. S.; Sadhu, K. M. *J. Am. Chem. Soc.* **1983**, *105*, 2077. (i) Matteson, D. S.; Beedle, E. C. *Tetrahedron Lett.* **1987**, *28*, 4499.

(19) Matteson, D. S.; Jesthi, P. K.; Sadhu, K. M. *Organometallics* **1984**, *3*, 1284.

(20) Korcek, S.; Watts, G. B.; Ingold, K. U. *J. Chem. Soc., Perkin Trans. 2* **1972**, 242.

Table 1. Inhibition of Subtilisin Carlsberg and α -Chymotrypsin by Acetamido Boronic Acids **1a–e**^a

inhibitor	R	inhibition constant K_I (μM)	
		subtilisin Carlsberg	α -chymotrypsin
 L-1a L-1b L-1c L-1d L-1e D-1a D-1b D-1c D-1d D-1e	H	78.5 \pm 4.1	no inhibition ^b
		1.22 \pm 0.03	3.80 \pm 0.13 ^c
		0.28 \pm 0.02	1.24 \pm 0.06
		0.15 \pm 0.01	1.20 \pm 0.05
		0.88 \pm 0.02	3.11 \pm 0.09.
	H	9300 \pm 350	no inhibition ^b
		126.2 \pm 5.2	79.9 \pm 3.3 ^d
		87.3 \pm 3.2	46.3 \pm 1.6
		91.3 \pm 5.4	5.76 \pm 0.23
		56.4 \pm 3.0	0.127 \pm 0.03
 2a 2b 2c 2d 2e	H	13000 ^e	not available
		257 ^e	481 ^f
		48 ^e	142 ^f
		19 ^e	52 ^f
		110 ^e	18.8 ^f

^a K_I values for both enzymes were determined in duplicate at pH 7.8 in 0.1 M KCl and at 25 °C. Initial rates for SC were measured at substrate (TAME) concentrations in the range of 0.075–0.15 M, inhibitor concentrations of 10^{-7} to 5.0×10^{-2} M, and an enzyme concentration of 2.0×10^{-7} M. Initial rates for CT were measured at substrate (NATEE) concentrations in the range of 1.5×10^{-4} to 3.0×10^{-3} M, inhibitor concentrations of 10^{-7} to 10^{-1} M and an enzyme concentration of 2.0×10^{-8} M. ^b No inhibition was observed at the concentration of the inhibitor, 5.0×10^{-2} M. ^c The reported value^{15b} is 2.1 μM . It was determined for the α -chymotrypsin-catalyzed hydrolysis of methyl hippurate at pH 7.5 and 25 °C. ^d The reported value^{15h} is 53 μM . ^e From reference 13b. ^f From reference 15e.

Inhibition Studies. The individual inhibition constants for each L- and D-acetamido boronic acid **1a–e** for SC and CT were determined using a pH-stat method and with *N-p*-tosyl-L-arginine methyl ester (TAME) as the standard substrate.^{2d} The boronic acids were added to the assay mixtures as their diethanolamine derivatives **6**, these being readily hydrolyzed by water under kinetic conditions to generate the corresponding boronic acid *in situ*.^{15f} The inhibitory activities of the boronic acids generated by *in situ* generation from their diethanolamine esters or anhydride forms were identical. Each boronic acid was found to be a competitive inhibitor, and the results are summarized in Table 1. For comparison purposes, and to evaluate the effect of the *N*-acetamido group itself, literature values^{13b,15e} for inhibition of SC and CT by the unsubstituted boronic acid parents of **1a–e** are also included in Table 1.

The (1*R*)-1-acetamido boronic acids L-**1a–e** are much more potent inhibitors of SC than the unsubstituted parent boronic acids **2a–e**, respectively. The largest increase of inhibitory power attributable to the introduction of an *R*-configuration

N-acetamido group is exhibited by the phenethyl derivative L-**1b**, with its K_I being 210-fold lower than that of **2b**. However, even the smallest, *N*-acetamido-induced, binding enhancement observed, that of 125-fold for the 1-naphthylethyl inhibitor L-**1e** over that of **2e**, is highly significant. Electronegative substituents in the *para*-position contribute very positively to inhibitor binding, as exemplified by the low K_I values of [2-(4-fluorophenyl)ethyl]- and [2-(4-chlorophenyl)ethyl]boronic acids (L-**1c,d**) relative to that of the phenethyl inhibitor L-**1b**. This is as expected from the additional electrostatic binding contributions resulting from the interactions of *para*-electronegative substituents of this type with the region of positive potential identified at the bottom of the S_1 -pocket of SC.^{13b} In contrast, for the enantiomeric compounds of the (*S*)-series D-**1a,b**, the effect of the *N*-acetamido group is minimal, and the inhibitory properties of these D-compounds are comparable to those of their unsubstituted parents **2a–e**. Some increases of binding efficiency (1.4–2.0-fold) when the *N*-acetamido is present are observed for the acetamido boronic acids D-**1a**, D-**1b**, and D-**1e**,

but inhibition by **D-1c** and **D-1d** is 1.8- and 4.8-fold worse than for the unsubstituted analogs **2c** and **2d**, respectively. It is evident that the configuration of the C-1 stereocenter is much more important than the properties of the substituent inducing the chirality.

The inhibition pattern for CT is quite different. Firstly, neither enantiomer of (1-acetamidoethyl)boronic acid (**1a**) inhibits CT, even at boronic acid concentrations of 50 mM. However, the CT inhibition trends for the (*R*)-inhibitors **L-1b-d** are similar to those for SC, with once more the (acetamidophenethyl)boronic acid **L-1b** manifesting the largest increase (127-fold) in binding enhancement relative to the parent, unsubstituted, boronic acid **2b**. Furthermore, the naphthyl acetamido compound **L-1e**, with its 6-fold reduction of K_1 over that of **2e**, again showed the lowest degree of substituent-induced augmentation of inhibition. However, in contrast to the minimal effects on SC inhibition of the acetamido substituent in the enantiomeric *D*-(*S*)-series, all the acetamido boronic acids **D-1b-e** are much better inhibitors of CT than their unsubstituted parents **2b-e**, respectively. Even the smallest (3-fold) decrease in K_1 observed for the 4-fluorophenethyl compound **D-1c** relative to **2c** is greater than any such trend for SC. Furthermore, unlike the SC situation, not of **D-1b-e** was a worse CT inhibitor than **2b-e**, respectively.

The most dramatic augmentation of inhibitory power arising from the introduction of the acetamido group is manifest in the inhibition of CT by the (*S*)-acetamido naphthyl boronic acid **D-1e**, whose K_1 of 0.127 μ M is extraordinarily low, and represents a remarkable 148-fold increase in binding efficiency relative to that of its progenitor **2e**. Most surprising was the fact that the *D*-enantiomer of **1e** was a 25-fold better inhibitor of CT than its *L*-counterpart, which represents a totally unexpected reversal of the high *L*-fidelity generally exhibited by this enzyme. The stereoselectivity reversal was rendered even more perplexing by the fact that, for SC, the normal *L*-over-*D* preference for **1e**-binding was retained by a large (64-fold) margin, and that no stereoselectivity reversals were evident for inhibitions of SC or CT by the other enantiomeric pairs of boronic acids **1b-d**. That the aromatic rings of **1b-d** possessed C_v symmetry while the naphthyl group of **1e** did not offered a possible basis for rationalizing the stereoselectivity reversal. In their EI complexes with SC and CT, the aromatic moieties of both *L*- and *D-1b-e* will occupy the hydrophobic S_1 -pocket, and the boronic acid OH's and the acetamido group will be directed toward the oxyanion hole and S_2 -pockets, respectively. Because of their symmetry, the orientations of the phenyl rings of **1b-d** in S_1 will not be affected by rotations about the C-2-to-aromatic σ -bonds. In contrast, for **1e**, rotations of the naphthyl group about this bond will give rise to distinct conformations, whose interactions with the individual S_1 -pockets of SC and CT could induce different enzyme inhibitor (EI) complexes with oppositely oriented naphthyl components, and for which binding of the *D*-enantiomer could become preferred. This concept is illustrated schematically in Figure 1. Further enlightenment on the basis of the observed stereospecificity reversal, and of the Table 1 binding trends, was sought using molecular modeling.

Molecular Modeling. Formulating appropriate molecular modeling protocols toward interpreting the Table 1 data was not straightforward because of the sometimes fickle nature of

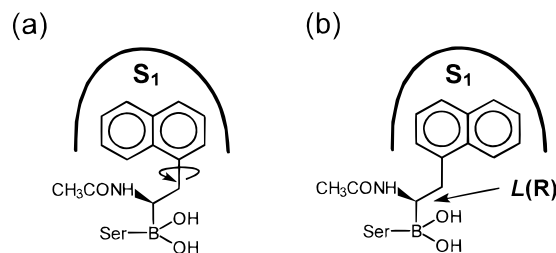


Figure 1. As a consequence of rotation about the σ -bond shown (\curvearrowright), different orientations can be envisaged for naphthyl groups in the S_1 -pockets of serine proteases, such as subtilisin Carlsberg and α -chymotrypsin, on formation of the preferred EI complexes. The left-oriented (a) and right-oriented (b) naphthyl conformations shown for the schematic EI complex of **L-4e** represent two such possibilities.

boronic acid binding to serine proteases. Boronic acids have been shown to be capable of forming tetrahedral complexes with either the active site serine or histidine residues.²¹ Generally the trend appears to be that good substrate analogs bind to serine and poor substrate analogs to histidine, although binding of a single inhibitor to give both a serine and a histidine adduct has been reported.²² However, because there is so far no X-ray structure of a serine protease-boronic acid complex involving histidine to use as a guide, only serine-bound boronic acid adducts, for which good X-ray data are available, were considered in the current molecular modeling study. Another consideration was our inability to overcome the problem posed by the unavailability of force field parameters for covalent B-N bonds.

Molecular graphics analyses in conjunction with molecular mechanics, molecular dynamics, and electrostatic calculations were applied in analyzing the Table 1 data. The high-resolution X-ray structures of SC^{4a} and CT^{5b} were energy-minimized using the Biosym "Discover" program and the boronic acid inhibitors *L*-(*R*)- and *D*-(*S*)-**1b-e** and then individually docked into the active site, using a CT-(phenylethyl)boronic acid X-ray structure^{5e} as a reference guide. Each EI complex was then subjected to energy minimization by Discover's molecular mechanics protocol, followed by molecular dynamics simulation for 20 ps. Analyses of the trajectories for SC showed that the *L*- and *D*-acetamido boronic acids **1b-d** oriented themselves at the active site in the normal^{5e} manner. For example, for *L*- and *D-1b*, the oxygen atoms of the two hydroxyl groups attached to the boron atom form hydrogen bonds to N ϵ of His64 and to the amide hydrogens of Asn155 and of the backbone NH of Ser221 of the oxyanion hole. The phenyl ring remains in the S_1 -pocket after the molecular dynamics simulation for both enantiomers. Also, the usual *L*-over-*D* stereoselectivity preference is maintained. The superiority of the *L*-enantiomer of **1b** as an SC inhibitor is due to the amide hydrogen of the 1-acetamido group forming a strong hydrogen bond with the carbonyl oxygen of Ser125 in the EI complex, whereas for its *D*-counterpart, this amide NH is directed toward the solvent and does not contribute to binding. Similarly, for the CT complexes with *L*- and *D-1b*, the phenyl ring remains in the S_1 -pocket, and there are strong interactions between the oxygens of the boronic acid with the backbone NH's of Gly193 and Ser195 of the oxyanion hole. Furthermore, the *L*-preference is again due to favorable hydrogen bonding, this time of the acetamido NH of *L-1b* with the carbonyl oxygen of Ser214, whereas the acetamido group of *D-1b* is once more oriented toward the solvent.

Most molecular modeling attention was directed toward interpreting the basis for the different stereoselectivities of SC and CT toward the enantiomeric naphthyl boronic acids *L*- and *D-1e*, focusing particularly on ascertaining if binding of the naphthyl

(21) (a) Tsilikounas, E.; Kettner, C. A.; Bachovchin, W. W. *Biochemistry* **1993**, *32*, 12651. (b) Tsilikounas, E.; Kettner, C. A.; Bachovchin, W. W. *Biochemistry* **1992**, *31*, 12839. (c) House, K. L.; Garber, A. R.; Dunlap, R. B.; Odom, J. D.; Hilvert, D. *Biochemistry* **1993**, *32*, 3468. (d) London, R. E.; Gabel, S. A. *J. Am. Chem. Soc.* **1994**, *116*, 2570. (e) Snow, R. J.; Bachovchin, W. W.; Barton, R. W.; Campbell, S. J.; Coutts, S. J.; Freeman, D. M.; Gutheil, W. G.; Kelly, T. A.; Kennedy, C. A.; et al. *J. Am. Chem. Soc.* **1994**, *116*, 10860.

(22) Zhong, S.; Haghjoo, K.; Kettner, C.; Jordan, F. *J. Am. Chem. Soc.* **1995**, *117*, 7048.

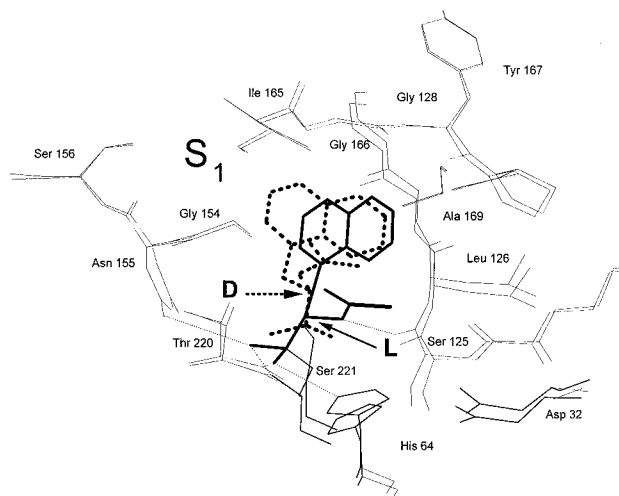


Figure 2. Superimposed energy-minimized EI complexes of L-(R)-**1e** (dark —) and D-(S)-**1e** (dark ···) respectively, in the active site of SC. Both naphthyl residues bind in S_1 . The oxyanions of the tetrahedral complexes derived from L-**1e** and D-**1e** are located in the oxyanion hole, with the negative charges on the boron oxygens well stabilized by hydrogen-bonding (light ···) with the peptide NH of Ser221, the side chain -NH₂ of Asn155, and the N ϵ of His64 for L-**1e**, but less well for the weaker inhibitor D-**1e**. In addition, a strong hydrogen bond is indicated between the backbone CO of Ser125 and the NH of the acetamido group of L-**1e**, but not for D-**1e**. All calculated hydrogen-bonding distances are given in the Experimental Section.

groups in different orientations of the Figure 1 type was an important determinant. The dimensions of the S_1 -pockets of both SC and CT are such that binding of the naphthyl substituents of **1e** in the two orientations shown in Figure 1 is allowed. In the initial dockings of L- and D-**1e** with SC, the left-orientation modes of Figure 1a directed the nonpolar C-5, -6, -7, and -8 region of the naphthalene ring toward the solvent, while with right-orientation binding (Figure 1b) these carbon atoms pointed inside toward the hydrophobic center of the S_1 -pocket. Molecular dynamics calculations on the SC complexes confirmed the right orientation to be favorable, and showed that left-orientation binding did not lead to stable EI complexes. Furthermore, the key hydrogen bond for L-stereoselectivity between the NH of the acetamido group of L-**1e** and the carbonyl oxygen of Ser125 is only present in the minimized right-orientation complex, and is absent for the analogous SC-D-**1e** complex in which the acetamido group points toward the solvent. The normal anion hole stabilization provided by Asn155 is not possible, and the tetrahedral intermediate anion is now hydrogen bonded to Ser221. The superimposed L- and D-**1e** complexes with SC are shown in Figure 2.

In contrast, binding of L- and D-**1e** into the active site of CT shows that the left orientation of the naphthyl group is now the more favorable. In this case, the naphthyl C-5, -6, -7, and -8 atoms are acceptably directed toward the Cys191-Cys220 disulfide bond and toward the backbone of the Gly216-Ser218 sequence (Figure 3). Moreover, the basis for the reversal of the normal L-stereoselectivity of CT is also revealed in that binding of D-**1e** becomes preferred over L-**1e** because of the strong hydrogen bond D-**1e** forms between the carbonyl oxygen of its acetamido group and the NH of His57. Conversely, analysis of the molecular dynamics trajectory for the complex of CT with L-**1e** provides no indication of such hydrogen bond stabilization between the acetamido carbonyl and its nearest NH neighbor, Ser214. Significantly, for the complexes of D-**1a-d** with CT, the molecular dynamics simulations do not identify an acetamido CO to histidine NH hydrogen bond, but instead indicate that in these cases the acetamido groups are exposed to the solvent. Thus, inhibitions of CT by the L-**1a-d** inhibitors

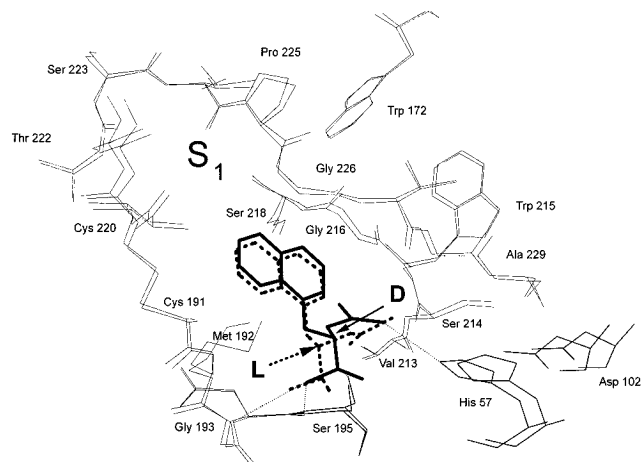


Figure 3. Superimposed energy-minimized EI complexes of D-(S)-**1e** (dark —) and L-(R)-**1e** (dark ···) respectively, in the active site of CT. The naphthyl groups of both inhibitors fit very similarly into the S_1 -pocket. The oxyanions of the tetrahedral complexes derived from D- and L-**1e** are located in the oxyanion hole, with the negative charges on the boron oxygens well stabilized by hydrogen-bonding (light ···) with the peptide NH's of Ser195 and Gly193 for both inhibitors. The excellence of the fits of the naphthyl groups into S_1 , and of the oxyanion hole stabilizations, accounts for the good inhibitory properties of both **1e** enantiomers. D-**1e** is the better inhibitor as a consequence of its ability to form an additional hydrogen bond between the CO of its acetamido group and the N ϵ of His57. All calculated hydrogen-bonding distances are given in the Experimental Section.

remain superior to those by their D-counterparts. However, the slightly better (3–9-fold) binding to CT of D-**1b-d** relative to that of **2b-d**, respectively, might reflect very weak hydrogen bond interactions of the D-**1e**-His57 type. The CT-L-**1e** complex is further disfavored by the somewhat adverse interactions of its naphthalene ring with the Cys191-Cys220 disulfide bond and with the Gly216-Ser218 backbone. These direct the acetamido group away from Ser214 and toward Val213. The calculated EI structures are shown in Figure 3. Interestingly, the calculated positions of the naphthalene rings of the **1e** enantiomers coincide more closely for the CT complexes than they do for those of SC (Figure 2). Attempts to correlate the calculated energies of the minimized structures, ranging from 1863 to 1914 kcal/mol for SC and from 2124 to 2179 kcal/mol for CT, with the differences in K_1 values of the Table 1 inhibitors were unsuccessful because of the variations in each complex of the positions of the active site region water molecules included in the simulations. With different water positions affecting the minimizations uniquely, we were unable to make valid comparisons of the final energies of the individual complexes.

The indication from molecular modeling that SC and CT can exhibit preferences for different inhibitor conformations raises the prospect of exploiting conformer preference as a means of tailoring enzyme stereoselectivity toward appropriate substrates, perhaps *via* strategies mimicking those applied in conformationally restricted enzyme inhibitor approaches to drug design. However, clearly many more data are needed before reliable guidelines for achieving such control can be formulated. Furthermore, once again it must be noted that a possibility remains that a change in boronic acid binding pattern, from the serine preference considered in the current modeling studies to one favoring histidine binding, could be at least partly responsible for the the K_1 and stereoselectivity trends observed. In this regard, the X-ray structures currently being determined of the SC and CT complexes with L- and D-**1b-e**²³ will provide

valuable insights, particularly into the concept of conformational selection by enzymes.

Experimental Section

General Methods. Unless otherwise stated, all reactions were performed under nitrogen using oven-dried glassware. Anhydrous reagents and solvents were prepared according to literature procedures.²⁴ Analytical thin layer chromatography was performed on Merck plates (silica gel F₂₅₄, 0.25 mm). Compounds that were not visualized by UV were detected by spraying with a mixture of ninhydrin (0.3 g) and acetic acid (3 mL) in ethanol (100 mL) followed by heating. Preparative flash column chromatography was performed using silica gel 60 (40–63 μ m), supplied by Toronto Research Chemicals Inc. Melting points were obtained on a Fisher-Johns melting point apparatus, and are uncorrected. Boiling points are of Kugelrohr distillations and are uncorrected. Optical rotations were measured with a Perkin-Elmer 243 B polarimeter equipped with a thermostated cell. Infrared (IR) spectra were determined in KBr pellets (for solids) and films (liquids) on a Nicolet 5DX FTIR spectrophotometer. ¹H and ¹³C NMR spectra were recorded on a Gemini 200 (at 200 and 50 MHz, respectively) spectrometer unless otherwise indicated. ¹H NMR chemical shifts are reported in parts per million relative to the CHCl₃ peak (δ = 7.24) with CHCl₃ as solvent, the DMSO peak (δ = 2.49) in DMSO-*d*₆, and the HOD peak (δ = 4.80) in D₂O. ¹³C NMR chemical shifts are reported in parts per million relative to the CHCl₃ peak (δ = 77.00) with CHCl₃ as solvent, the DMSO peak (δ = 39.50) in DMSO-*d*₆ and external dioxane (δ = 66.50) in D₂O as solvent. Mass spectra were measured on a Bell and Howell 21-490 (low resolution) or an AEI MS3074 (high resolution) instrument. Elemental analyses were by Galbraith Laboratories, Knoxville, TN.

Reagent grade chemicals were purchased from Aldrich. Subtilisin Carlsberg (SC; EC 3.4.21.14), α -chymotrypsin (CT; EC 3.4.21.1), *N*-*p*-tosyl-L-arginine methyl ester (TAME), and *N*-acetyl-L-tyrosine ethyl ester (NATEE) were purchased from Sigma Chemical Co., St. Louis, MO. The concentrations of SC and α -chymotrypsin were determined by assaying the rates of hydrolysis of standard solutions of succinyl-L-Ala-L-Ala-L-Pro-L-Phe-*p*-nitroanilide²⁵ and *p*-nitrophenyl acetate,²⁶ respectively.

Preparations of Inhibitors. L-Series. The same basic, Scheme 1, procedure was used for each inhibitor, with the following being representative.

[(1*R*)-1-Acetamido-2-(1-naphthyl)ethyl]boronic Acid (1-1e). A solution of (1-naphthylmethyl)magnesium chloride, obtained from 1-naphthylmethyl chloride (8.8 g, 50 mmol) and activated Mg (1.2 g, 50 mmol) in dry Et₂O (50 mL) at 20 °C, was added slowly (over 15 min) at –70 °C to a solution of trimethyl borate (5.68 mL, 50 mmol) in dry Et₂O (150 mL) and the resulting white suspension stirred for 1 h at –70 °C. The mixture was then allowed to warm to 20 °C and stirred for a further 10 h. Aqueous H₂SO₄ (10%, 50 mL) was then slowly added at 0 °C, the Et₂O layer separated, and the aqueous phase extracted with Et₂O (3 \times 50 mL). The combined ethereal phases were washed with water and then extracted with 2 M aqueous KOH (3 \times 50 mL). The aqueous extracts were combined, washed with Et₂O, cooled to 0 °C, and then acidified to pH 2 with 10% aqueous H₂SO₄ and saturated with NaCl. Et₂O was added (50 mL), the Et₂O layer separated, and the aqueous phase extracted further with Et₂O (2 \times 50 mL). The combined organic phases were dried (MgSO₄) and filtered, and (+)-pinanediol (4.25 g, 25 mmol) was added at 20 °C to the stirred solution. The course of the reaction was followed by TLC, and was generally complete in 1 h, although sometimes addition of more pinanediol was needed to complete the reaction. The mixture was then filtered, concentrated *in vacuo*, and Kugelrohr distilled to give (+)-pinanediol (1-naphthylmethyl)boronate (**3e**; 6.24 g, 39%), bp 160–165 °C (0.2 mmHg), [α]_D²⁵ = +24.4 (*c* 6.52, toluene). IR (film): ν 2926, 1458, 1282, 1238 cm⁻¹. ¹H NMR (CDCl₃): δ 0.79 (s, 3 H),

1.06 (d, *J* = 10.58 Hz, 1 H), 1.25 (s, 3 H), 1.36 (s, 3 H), 1.70–2.31 (m, 5 H), 2.75 (s, 2 H), 4.24 (dd, *J* = 2.02 and 8.73 Hz, 1 H), 7.36–8.07 (m, 7 H). ¹³C NMR (CDCl₃): δ 17.36, 23.74, 26.23, 26.82, 28.40, 35.22, 37.92, 39.25, 51.09, 77.89, 85.86, 124.59, 125.43, 125.50, 125.83, 125.90, 126.46, 128.64, 132.47, 133.92, 135.76.

A solution of CH₂Cl₂ (1.02 mL, 16 mmol) in dry THF (30 mL) was cooled to –100 °C in an EtOH/liquid N₂ bath and stirred magnetically during the dropwise addition of *n*-BuLi (6.9 mL of a 1.6 M solution in hexane, 11 mmol) by running the BuLi solution down the cold wall of the reaction flask. After about half of the BuLi had been added, a white precipitate of LiCHCl₂ became evident. Twenty minutes after all the BuLi had been added, (+)-pinanediol (1-naphthylmethyl)boronate (**3e**; 3.2 g, 10 mmol) in dry Et₂O (10 mL) was added in one portion. The solution was stirred at –100 °C for 10 min, after which a portion of rigorously dried ZnCl₂²⁷ (0.56 g, 4.1 mmol) was added. The mixture, still in the cooling bath, was then allowed to warm slowly to 20 °C and stirred overnight. The solution was concentrated by rotary evaporation (bath temperature <30 °C), and the residue was dissolved in Et₂O (25 mL), treated with silica gel (10 g), and then triturated with hexanes (25 mL). The resulting mixture was loaded on a short silica gel column (length 10 cm, diameter 3.5 cm) and eluted with hexanes/Et₂O (1:1, 300 mL). The eluents were concentrated on a rotary evaporator (bath temperature <30 °C) to give (+)-pinanediol [(1*S*)-1-chloro-2-(1-naphthyl)ethyl]boronate (**4e**; 2.97 g, 81%) as an oil, [α]_D²⁵ = +22.1 (*c* 2.13, toluene). IR (film): ν 2924, 1455, 1408, 1240 cm⁻¹. ¹H NMR (CDCl₃): δ 0.83 (s, 3 H), 1.06 (d, *J* = 11.00 Hz, 1 H), 1.28 (s, 3 H), 1.35 (s, 3 H), 1.83–2.34 (m, 5 H), 3.16 (m, 2 H), 3.67 (t, *J* = 8.06 Hz, 1 H), 4.35 (dd, *J* = 1.91 and 8.87 Hz, 1 H), 7.28 (m, 5 H). ¹³C NMR (CDCl₃): δ 23.62, 25.94, 26.69, 27.96, 34.82, 37.20, 37.91, 39.04, 41.62, 50.89, 78.34, 86.64, 123.44, 125.30, 125.59, 126.16, 127.48, 127.65, 128.89, 131.82, 133.93, 134.21.

A solution of lithium hexamethyldisilazane was prepared at –78 °C from hexamethyldisilazane (1.84 mL, 8.70 mmol) and *n*-BuLi (5.25 mL of a 1.6 M solution in hexane, 8.40 mmol) in THF (15 mL). (+)-Pinanediol [(1*S*)-1-chloro-2-(1-naphthyl)ethyl]boronate (**4e**; 2.68 g, 7.30 mmol) was added at –78 °C to the stirred solution and the mixture then allowed to warm to 20 °C and stirred for 10 h. The mixture was then cooled to –78 °C, and Ac₂O (2.82 mL, 25.5 mmol) and CH₃-COOH (0.53 mL, 9.3 mmol) were added dropwise with stirring. After the mixture had been stirred overnight at 20 °C, the solvent was removed on a rotary evaporator and EtOAc (30 mL) and H₂O (30 mL) were added. The aqueous layer was separated and extracted with EtOAc (2 \times 20 mL). The combined EtOAc layers were washed successively with 5% aqueous NaHCO₃ (25 mL), H₂O (25 mL), and brine (25 mL) and dried (MgSO₄). The solution was concentrated under vacuum, and the residue flash-chromatographed on a silica gel column with 5% MeOH in Et₂O elution. The eluents were rotary evaporated and the product recrystallized to constant rotation from EtOAc/CHCl₃ to afford (+)-pinanediol [(1*R*)-1-acetamido-2-(1-naphthyl)ethyl]boronate (**5e**; 1.88 g, 66%), mp 235–239 °C, [α]_D²⁵ = –55.5 (*c* 2.88, CHCl₃). IR (KBr): ν 3173, 1606, 1561, 1170 cm⁻¹. ¹H NMR (CDCl₃): δ 0.88 (s, 3 H), 1.29 (s, 3 H), 1.42 (s, 3 H), 1.55 (d, *J* = 10.26 Hz, 1 H), 1.86–2.06 (m, 3 H), 1.98 (s, 3 H), 2.18–2.36 (m, 2 H), 3.09–3.20 (m, 2 H), 3.46 (q, *J* = 10.53 Hz, 1 H), 4.27 (dd, *J* = 2.03 and 8.49 Hz, 1 H), 6.16 (br s, 1 H, variable position), 7.27–8.06 (m, 7 H). ¹³C NMR (DMSO-*d*₆): δ 17.14, 23.99, 25.99, 26.09, 27.24, 29.49, 34.83, 36.72, 37.58, 39.65, 43.84, 52.23, 75.43, 81.88, 123.71, 125.68, 125.81, 126.07, 126.72, 127.17, 128.95, 131.74, 133.87, 137.04, 175.24.

To a stirred solution of BCl₃ (15 mL of a 1 M solution in CH₂Cl₂) in CH₂Cl₂ (30 mL) at –78 °C was added solid (+)-pinanediol [(1*R*)-1-acetamido-2-(1-naphthyl)ethyl]boronate (**5e**; 1.27 g, 3.25 mmol). The mixture was stirred at –78 °C for 1 h and the cooling bath then removed. The mixture was evaporated under vacuum (0.1 mmHg) while evolving BCl₃ and CH₂Cl₂ were condensed in a trap at –78 °C. Water (30 mL) and Et₂O (70 mL) were added, and the aqueous phase was separated and washed with Et₂O (3 \times 20 mL). Lyophilization of the aqueous phase yielded crude **1e**, which was freed from the boric acid contaminant by successive treatments with MeOH (50 mL) followed by distillation until the distillate showed no green boron color in the flame when a drop was ignited. The remaining MeOH was

(24) Perin, D. D.; Armarego, W. L. F.; Perrin, D. R. *Purification of Laboratory Chemicals*; Pergamon Press: New York, 1980.

(25) (a) Del Mar, E. G.; Largam, C.; Brodrick, J. W.; Goekas, M. C. *Anal. Biochem.* **1979**, *99*, 316. (b) Russell, A. J.; Thomas, P. G.; Fersht, A. R. *J. Mol. Biol.* **1987**, *193*, 803.

(26) (a) Kézdy, F. J.; Kaiser, E. T. *Methods Enzymol.* **1970**, *19*, 3. (b) Ottensen, M.; Svendsen, I. In *Methods of Enzymatic Analysis*, Bertram, H. V., Ed.; 1984; Vol. 5, p 159.

(27) Zinc chloride was dried at 130 °C and 0.05 mmHg with magnetic stirring for 12 h.

removed by distillation under vacuum, and water (30 mL) and Et₂O (30 mL) were added to the residue. The aqueous phase was separated, washed with Et₂O (3 × 20 mL), and then lyophilized to give [(1*R*)-1-acetamido-2-(1-naphthyl)ethyl]boronic acid (**1e**; 0.36 g, 43%) as the trimeric anhydride, mp 166–171 °C, [α]²³_D = -142.3 (c 1.22, CH₃-OH). IR (KBr): ν 3700–2800, 1631, 1248 cm⁻¹. ¹H NMR (CD₃-OD): δ 2.13 (s, 3 H), 3.02 (m, 2 H), 3.40 (m, 1 H), 7.35–8.07 (m, 7 H). ¹³C NMR (CD₃OD): δ 16.41, 34.68, 48.87 (br), 124.55, 126.54, 126.63, 126.93, 127.67, 128.03, 129.87, 133.18, 135.55, 137.51, 178.43. HRMS: calcd for C₁₂H₁₂ B₃N₃O₆ 717.3353, found 717.3358.

The target **L-1e** was further characterized as its diethanolamine derivative **L-6e** as follows: diethanolamine (0.21 g, 2 mmol) in 2-propanol (5 mL) was added with stirring at 20 °C to a solution of [(1*R*)-1-acetamido-2-(1-naphthyl)ethyl]boronic acid (**L-1e**; 514 mg, 2 mmol) in *i*-PrOH (5 mL). The solution was stirred for a further 1 h, the *i*-PrOH then rotary evaporated, and the residue dissolved in CH₂-Cl₂ (20 mL). Anhydrous MgSO₄ and activated charcoal were added, and the mixture was stirred for 10 h. Filtration through Celite, followed by concentration under vacuum, afforded a white solid which was further purified by repeated precipitation from CH₂Cl₂ with Et₂O to yield diethanolamine [(1*R*)-1-acetamido-2-(1-naphthyl)ethyl]boronate (**L-6e**; 228 mg, 35%), mp 240–245 °C dec, [α]²³_D = -129.6 (c 0.55, CH₂Cl₂). IR (KBr): ν 3254, 3085, 1630, 1218 cm⁻¹. ¹H NMR (CDCl₃): δ 1.89 (s, 3 H), 2.52–2.74 (m, 3 H), 3.07–3.24 (m, 3 H), 3.34–3.83 (m, 5H), 6.76 (br t, 1 H), 7.20–8.13 (m, 8H). ¹³C NMR (CDCl₃): δ 23.26, 31.87, 46.65 (br), 50.67, 50.85, 63.04 (double peak), 123.88, 125.33, 125.45, 125.60, 125.76, 126.47, 128.61, 132.03, 133.89, 137.59, 172.18. Anal. Calcd for C₁₈H₂₃BN₂O₃: C, 66.28; H, 7.11; N, 8.59. Found: C, 66.21; H, 7.15; N, 8.49.

The other inhibitors in this (1*R*)-configuration series, **L-1a–d**, were prepared on the same scale by the above procedures, *via* the Scheme 1 intermediates, as follows.

[(1*R*)-1-Acetamidoethyl]boronic Acid (L-1a). (+)-Pinanediol methylboronate (**3a**; 41%, obtained using purchased methylmagnesium bromide), bp 60–65 °C (3 mmHg), [α]²³_D = +37.0 (c 3.58 CHCl₃) (lit.^{18d} bp 37–41 °C (0.25 mmHg)). IR (film): ν 2931, 1280, 1078 cm⁻¹. ¹H NMR (CDCl₃): δ 0.26 (s, 3 H), 0.81 (s, 3 H), 1.09 (d, *J* = 10.67 Hz, 1 H), 1.26 (s, 3 H), 1.36 (s, 3 H), 1.86–2.30 (m, 5 H), 4.23 (dd, *J* = 1.85 and 8.69 Hz, 1 H). ¹³C NMR (CDCl₃): δ 23.77, 26.22, 26.87, 28.45, 35.27, 37.93, 39.33, 51.14, 77.55, 85.36 (C next to B not seen). (+)-Pinanediol [(1*S*)-1-chloroethyl]boronate (**L-4a**; 79%), bp 58–60 °C (0.1 mmHg), [α]²³_D = +33.6 (c 2.35, toluene). IR (film): ν 2928, 1456, 1412, 1394, 1380, 1339, 1284, 1240, 1076, 1006 cm⁻¹. ¹H NMR (CDCl₃): δ 0.82 (s, 3 H), 1.14 (d, *J* = 10.94 Hz, 1 H), 1.27 (s, 3 H), 1.40 (s, 3 H), 1.55 (d, *J* = 7.57 Hz, 3 H), 1.83–2.34 (m, 5 H), 3.55 (q, *J* = 7.51 Hz, 1 H), 4.34 (dd, *J* = 1.91 and 8.83 Hz, 1 H). ¹³C NMR (CDCl₃): δ 20.37, 23.75, 26.07, 26.23, 26.81, 28.21, 35.07, 38.06, 39.15, 51.05, 78.52, 86.73. (+)-Pinanediol [(1*R*)-1-acetamidoethyl]boronate (**5a**; 73%), mp 196–198 °C, [α]²³_D = -21.24 (c 1.13, CHCl₃) (lit.¹⁹ mp 197–198 °C, [α]²¹₅₄₆ = -25.50 (c 2.9, CHCl₃)). IR (KBr): 3182, 1612, 1286, 1082 cm⁻¹. ¹H NMR (CDCl₃): δ 0.82 (s, 3 H), 1.08 (d, *J* = 7.24 Hz, 3 H), 1.22 (s, 3 H), 1.34 (s, 3 H), 1.43 (d, *J* = 9.40 Hz, 1 H), 1.70–2.28 (m, 5 H), 1.99 (s, 3 H), 2.53 (q, *J* = 7.32 Hz, 1 H), 4.14 (dd, *J* = 2.07 and 8.47 Hz, 1 H), 9.20 (br s, 1 H, variable positions). ¹³C NMR (CDCl₃): δ 15.87, 16.78, 23.89, 26.34, 27.08, 29.13, 36.77, 37.87, 39.28, 39.94, 52.38, 75.63, 82.76, 174.75; [(1*R*)-1-acetamidoethyl]boronic acid (**L-1a**; 91%), mp 185–188 °C, [α]²³_D = -82.8 (c 0.39, H₂O). IR (KBr): ν 3700–2800, 1630, 1540, 1429, 1383, 1240, 807, cm⁻¹. ¹H NMR (D₂O) δ 1.10 (d, *J* = 7.32 Hz, 3 H), 2.16 (s, 3 H), 2.70 (q, *J* = 7.28 Hz, 1 H). ¹³C NMR (D₂O, CH₃CN as internal standard, δ 1.60 for CH₃): δ 15.23, 16.76, 43.57 (br), 177.37. The HRMS was not obtainable, so **L-1a** was further characterized as diethanolamine [(1*R*)-1-acetamidoethyl]boronate (**6a**; 49%), mp 175–176 °C, [α]²³_D = -22.4 (c 0.90, CH₂Cl₂). IR (KBr): ν 3307, 3115, 1626, 1309, 1099 cm⁻¹. ¹H NMR (CDCl₃) δ 1.20 (d, *J* = 7.61 Hz, 3 H), 1.93 (s, 3 H), 2.71–2.78 (m, 2 H), 2.91–3.02 (m, 2 H), 3.24–3.41 (m, 1 H), 3.78–4.01 (m, 4 H), 5.70 (br s, 1 H), 7.43 (br s, 1 H). ¹³C NMR (CDCl₃): δ 15.57, 23.15, 39.70 (br), 50.67, 51.02, 62.95, 63.10, 171.10. Anal. Calcd for C₈H₁₇BN₂O₃: C, 48.03; H, 8.57. Found: C, 47.81; H, 8.59.

[(1*R*)-1-Acetamido-2-phenylethyl]boronic Acid (L-1b). (+)-Pinanediol (phenylmethyl)boronate (**3b**; 44%), bp 110–112 °C (0.2 mmHg), [α]²³_D +31.6 (c 6.30 toluene) (lit.^{18c} bp 108–110 °C (0.1

mmHg), [α]²³_D = +31.8 (c 6.00, toluene). IR (film): ν 2928, 1282, 1238, 1076 cm⁻¹. ¹H NMR (CDCl₃): δ 0.85 (s, 3 H), 1.08 (d, *J* = 10.80 Hz, 1 H), 1.30 (s, 3 H), 1.41 (s, 3 H), 1.80–2.39 (m, 5 H), 2.37 (s, 2 H), 4.30 (dd, *J* = 1.82 and 8.67 Hz, 1 H), 7.15–7.38 (m, 5 H). ¹³C NMR (CDCl₃): δ 20.00, 24.40, 26.16, 26.83, 28.37, 35.23, 37.91, 39.26, 51.13, 77.82, 85.71, 124.90, 128.33, 129.00, 138.85. (+)-Pinanediol [(1*S*)-1-chloro-2-phenylethyl]boronate (**4b**; 92%), recrystallized from EtOH, mp 46–47 °C, [α]²³_D = +25.0 (c 2.35, toluene). IR (KBr): ν 2930, 1239, 1077, 1008 cm⁻¹. ¹H NMR (CDCl₃): δ 0.83 (s, 3 H), 1.06 (d, *J* = 11.00 Hz, 1 H), 1.28 (s, 3 H), 1.35 (s, 3 H), 1.83–2.34 (m, 5 H), 3.16 (m, 2 H), 3.67 (t, *J* = 8.06 Hz, 1 H), 4.35 (dd, *J* = 1.91 and 8.87 Hz, 1 H), 7.28 (m, 5 H). ¹³C NMR (CDCl₃): δ 23.70, 25.98, 26.76, 28.10, 34.91, 37.98, 39.09, 40.17, 42.93, 50.93, 78.39, 86.71, 126.78, 128.41, 129.24, 138.49. (+)-Pinanediol [(1*R*)-1-acetamido-2-phenylethyl]boronate (**L-5b**; 81%), mp 190–192 °C, [α]²³_D = -82.5 (c 4.90, CHCl₃) (lit.^{15b} mp 185–186 °C, [α]²³_D = -82.4 (c 5.00, CHCl₃)). IR (KBr): ν 3183, 3072, 1609, 1161 cm⁻¹. ¹H NMR (CDCl₃): δ 0.87 (s, 3 H), 1.28 (s, 3 H), 1.40 (s, 3 H), 1.43 (d, *J* = 9.40 Hz, 1 H), 1.82–2.34 (m, 5 H), 2.04 (s, 3 H), 2.72 (dd, *J* = 12.29 Hz and 14.85 Hz, 1 H), 2.97 (m, 2 H), 4.24 (dd, *J* = 2.04 and 8.52 Hz, 1 H), 6.30 (br s, 1 H, variable positions), 7.27 (m, 5 H). ¹³C NMR (CDCl₃): δ 17.75, 23.83, 25.96, 26.97, 28.91, 36.09, 36.96, 37.76, 39.64, 44.51, 51.98, 75.91, 83.09, 126.12, 128.41, 128.77, 140.46, 174.68. [(1*R*)-1-Acetamido-2-phenylethyl]boronic acid (**L-1b**; 83%), mp 145–147 °C, [α]²³_D = -185.2 (c 1.33, H₂O) (lit.^{15b} [α]²²_D (as anhydride) = -195.8 (c 0.60, H₂O)). IR (KBr): ν 3700–2800, 1635, 1268 cm⁻¹. ¹H NMR (D₂O) δ 2.11 (s, 3 H), 2.60 (dd, *J* = 12.64 and 15.57 Hz, 1 H), 2.88 (m, 2 H), 7.30–7.43 (m, 5H). ¹³C NMR (D₂O, CH₃OH as internal standard, δ 49.90): δ 17.03, 37.18, 50.59 (br), 127.56, 129.90, 130.05, 141.80, 177.94. HRMS: calcd for C₃₀H₃₆ B₃N₃O₆ 567.2883, found 567.2859. Diethanolamine [(1*R*)-1-acetamido-2-phenylethyl]boronate (**L-6b**; 42%), mp 177–178 °C, [α]²³_D = -32.8 (c 0.96, CH₂Cl₂); IR (KBr): ν 3449, 3394, 1620, 1105, 1079 cm⁻¹. ¹H NMR (CDCl₃) δ 1.86 (s, 3 H), 2.71–2.86 (m, 3 H), 3.10–3.23 (m, 3 H), 3.32–3.56 (m, 1 H), 3.76–4.10 (m, 4 H), 5.87 (br s, 1 H), 7.20–7.34 (m, 5 H), 7.64 (br s, 1 H). ¹³C NMR (CDCl₃): δ 23.14, 31.80, 46.90 (br), 50.69, 51.01, 63.09 (double peak), 125.62, 128.16, 128.12, 141.52, 172.07. HRMS: calcd for C₁₄H₂₁BN₂O₃ 276.1645, found 276.1646.

[(1*R*)-1-Acetamido-2-(1-fluorophenyl)ethyl]boronic Acid (L-1c). (+)-Pinanediol [(4-fluorophenyl)methyl]boronate (**3c**; 44%), bp 120–122 °C (0.35 mmHg), [α]²³_D = +29.5 (c 6.60 toluene). IR (film): ν 2922, 1286, 830 cm⁻¹. ¹H NMR (CDCl₃): δ 0.80 (s, 3 H), 1.02 (d, *J* = 10.62 Hz, 1 H), 1.25 (s, 3 H), 1.35 (s, 3 H), 1.76–2.36 (m, 5 H), 2.28 (s, 2 H), 4.25 (dd, *J* = 1.91 and 8.59 Hz, 1 H), 6.90 (t, *J* = 8.50 Hz, 2 H), 7.11 (dd, *J* = 5.51 and 8.53 Hz, 2 H). ¹³C NMR (CDCl₃): δ 18.39, 23.73, 26.18, 26.82, 28.37, 35.25, 37.95, 39.27, 51.13, 77.89, 85.84, 115.00 (d, *J* = 21.1 Hz), 130.24 (d, *J* = 7.6 Hz), 34.37 (d, *J* = 2.2 Hz), 160.97 (d, *J* = 242.8 Hz). (+)-Pinanediol [(1*S*)-1-chloro-2-(4-fluorophenyl)ethyl]boronate (**4c**; 87%), mp 64–65 °C, [α]²³_D = +25.5 (c 2.19, toluene). IR (KBr): ν 2920, 1285, 832 cm⁻¹. ¹H NMR (CDCl₃): δ 0.83 (s, 3 H), 1.04 (d, *J* = 10.62 Hz, 1 H), 1.29 (s, 3 H), 1.36 (s, 3 H), 1.82–2.36 (m, 5 H), 3.13 (m, 2 H), 3.62 (t, *J* = 7.98 Hz, 1 H), 4.35 (dd, *J* = 2.04 and 8.71 Hz, 1 H), 6.98 (t, *J* = 8.10 Hz, 2 H), 7.23 (dd, *J* = 5.49 and 8.06 Hz, 2 H); ¹³C NMR (CDCl₃): δ 23.69, 25.99, 26.75, 28.12, 34.91, 38.00, 39.10, 39.30, 42.99 (br), 50.94, 78.46, 86.81, 115.11 (d, *J* = 21.2 Hz), 131.20 (d, *J* = 7.9 Hz), 136.23 (d, *J* = 3.0 Hz), 161.96 (d, *J* = 245.3 Hz). (+)-Pinanediol [(1*R*)-1-acetamido-2-(4-fluorophenyl)ethyl]boronate (**5c**; 83%), recrystallized from EtOAc, mp 139–140 °C, [α]²³_D = -68.4 (c 4.62, CHCl₃). IR (KBr): ν 3184, 3076, 1608, 1160 cm⁻¹. ¹H NMR (CDCl₃): δ 0.82 (s, 3 H), 1.24 (s, 3 H), 1.32 (d, *J* = 10.43 Hz, 1 H), 1.34 (s, 3 H), 1.75–2.34 (m, 5 H), 2.00 (s, 3 H), 2.66 (dd, *J* = 11.76 and 14.98 Hz, 1 H), 2.90 (m, 2 H), 4.18 (dd, *J* = 2.20 and 8.79 Hz, 1 H), 6.25 (br s, 1 H, variable positions), 6.95 (t, *J* = 8.73 Hz, 2 H), 7.13 (dd, *J* = 5.50 and 8.68 Hz, 2 H); ¹³C NMR (CDCl₃): δ 17.92, 23.82, 25.94, 26.97, 28.92, 36.06, 36.18, 37.81, 39.64, 44.32 (br), 52.00, 76.1, 83.3, 115.12 (d, *J* = 21.1 Hz), 130.23 (d, *J* = 7.8 Hz), 136.01 (d, *J* = 3.2 Hz), 161.50 (d, *J* = 244.7 Hz), 174.65. [(1*R*)-1-Acetamido-2-(1-fluorophenyl)ethyl]boronic acid (**L-1c**; 68%), mp 132–135 °C, [α]²³_D = -156.8 (c 0.91, H₂O). IR (KBr): ν 3700–2800, 1630, 1222, 824 cm⁻¹. ¹H NMR (D₂O): δ 2.10 (s, 3 H), 2.54 (dd, *J* = 12.72 and 15.57 Hz, 1 H), 2.82 (m, 2 H), 7.08 (t, *J* = 8.83 Hz, 2 H), 7.28 (dd, *J* = 5.64 and 8.80

Hz, 2H). ^{13}C NMR (D_2O): δ 16.99, 36.30, 50.47 (br), 116.25 (d, $J = 21.1$ Hz), 131.47 (d, $J = 8.0$ Hz), 137.29 (d, $J = 2.8$ Hz), 162.50 (d, $J = 241.9$ Hz), 178.09. Anal. Calcd for $\text{C}_{10}\text{H}_{13}\text{BFNO}_3$: C, 53.38; H, 5.82; N, 6.22. Found: C, 53.25; H, 5.66; N, 6.05. Diethanolamine [(1*R*)-1-acetamido-2-(4-fluorophenyl)ethyl]boronate (**L-6c**; 56%), mp 197–200 °C, $[\alpha]_D^{23} = -29.6$ (c 0.68, CH_2Cl_2). IR (KBr): ν 3381, 3085, 1622, 1112, 826 cm^{-1} . ^1H NMR (CDCl_3): δ 1.82 (s, 3 H), 2.65–2.82 (m, 3 H), 2.99–3.12 (m, 3 H), 3.29–3.46 (m, 1 H), 3.72–4.01 (m, 4 H), 5.85 (br d, $J = 5.13$ Hz, 1 H), 6.92 (t, $J = 8.76$ Hz, 2 H), 7.12 (dd, $J = 5.49$ and 8.58 Hz, 2H), 7.51 (br s, 1 H); ^{13}C NMR (CDCl_3): δ 23.12, 31.05, 46.71 (br), 50.71, 51.02, 63.12 (double peak), 114.87 (d, $J = 21.0$ Hz), 129.73 (d, $J = 7.7$ Hz), 137.08 (d, $J = 3.1$ Hz), 161.15 (d, $J = 243.2$ Hz), 172.01. Anal. Calcd for $\text{C}_{14}\text{H}_{20}\text{BFN}_2\text{O}_3$: C, 57.17; H, 6.85; B, 3.68; N, 9.52. Found: C, 56.75; H, 6.98; B, 3.47; N, 9.26.

[(1*R*)-1-Acetamido-2-(1-chlororophenyl)ethyl]boronic Acid (L-1d). (+)-Pinanediol [(4-chlorophenyl)methyl]boronate (**3d**; 40%), recrystallized from Et_2O /hexanes, mp 59 °C, $[\alpha]_D^{23} = +25.9$ (c 6.06 toluene). IR (KBr): ν 2912, 1283, 1078, 806 cm^{-1} . ^1H NMR (CDCl_3): δ 0.81 (s, 3 H), 1.01 (d, $J = 10.62$ Hz, 1 H), 1.26 (s, 3 H), 1.36 (s, 3 H), 1.99–2.33 (m, 5 H), 2.29 (s, 2 H), 4.26 (d, $J = 8.57$ Hz, 1 H), 7.10 (d, $J = 8.22$ Hz, 2 H), 7.19 (d, $J = 8.24$ Hz, 1 H). ^{13}C NMR (CDCl_3): δ 18.42 (br), 23.76, 26.22, 26.84, 28.39, 35.24, 37.98, 39.27, 51.13, 77.95, 85.94, 128.44, 130.36, 130.71, 137.43. (+)-Pinanediol [(1*S*)-1-chloro-2-(4-chlorophenyl)ethyl]boronate (**L-4d**; 95%), recrystallized from EtOH, mp 92–93 °C, $[\alpha]_D^{23} = +23.5$ (c 2.20, toluene). IR (KBr): ν 2910, 1284, 1075, 805 cm^{-1} . ^1H NMR (CDCl_3): δ 0.84 (s, 3 H), 1.05 (d, $J = 10.62$ Hz, 1 H), 1.29 (s, 3 H), 1.37 (s, 3 H), 1.83–2.34 (m, 5 H), 3.12 (m, 2 H), 3.62 (t, $J = 7.88$ Hz, 1 H), 4.36 (d, $J = 8.71$ Hz, 1 H), 7.20 (d, $J = 8.36$ Hz, 2 H), 7.28 (d, $J = 8.36$ Hz, 2 H). ^{13}C NMR (CDCl_3): δ 23.71, 26.02, 26.77, 28.15, 34.92, 38.02, 39.11, 39.41, 42.38, 50.96, 78.51, 86.88, 128.54, 130.68, 132.65, 137.04. (+)-Pinanediol [(1*R*)-1-acetamido-2-(4-chlorophenyl)ethyl]boronate (**5d**; 79%), mp 152–153 °C, $[\alpha]_D^{23} = -78.6$ (c 5.36, CHCl_3). IR (KBr): ν 3170, 3075, 1606, 1066 cm^{-1} . ^1H NMR (CDCl_3): δ 0.85 (s, 3 H), 1.25 (s, 3 H), 1.34 (d, $J = 9.77$ Hz, 1 H), 1.36 (s, 3 H), 1.77–2.31 (m, 5 H), 2.01 (s, 3 H), 2.67 (dd, $J = 11.96$ and 15.02 Hz, 1 H), 2.91 (m, 2 H), 4.19 (dd, $J = 2.20$ and 8.71 Hz, 1 H), 6.43 (br s, 1 H, variable positions), 7.11 (d, $J = 8.42$ Hz, 2 H), 7.28 (d, $J = 8.42$ Hz, 2H). ^{13}C NMR (CDCl_3): δ 17.83, 23.83, 25.99, 26.98, 28.95, 36.10, 36.39, 37.81, 39.63, 44.40, 52.00, 75.85, 83.28, 128.52, 130.17, 131.91, 138.95, 174.77. [(1*R*)-1-Acetamido-2-(1-chlororophenyl)ethyl]boronic acid (**L-1d**; 79%), mp 140–143 °C, $[\alpha]_D^{23} = -165.8$ (c 0.63, H_2O). IR (KBr): ν 3700–2800, 1625, 1266, 805 cm^{-1} . ^1H NMR (D_2O): δ 2.11 (s, 3 H), 2.54 (dd, $J = 12.82$ and 15.47 Hz, 1 H), 2.83 (m, 2 H), 7.26 (d, $J = 8.42$ Hz, 2 H), 7.37 (d, $J = 8.42$ Hz, 2H). ^{13}C NMR (D_2O): δ 17.28, 36.73, 50.12 (br), 129.44, 131.30, 132.34, 140.11, 177.66. HRMS (FAB): calcd for $\text{C}_{10}\text{H}_{13}\text{BClNO}_3$: 669.1714, found 669.1755. Diethanolamine [(1*R*)-1-acetamido-2-(4-chlorophenyl)ethyl]boronate (**L-6d**; 48%), mp 218–221 °C, $[\alpha]_D^{23} = -25.4$ (c 0.68, CH_2Cl_2). IR (KBr): ν 3316, 3108, 1637, 1274, 806 cm^{-1} . ^1H NMR (CDCl_3): δ 1.84 (s, 3 H), 2.66–2.80 (m, 3 H), 3.01–3.16 (m, 3 H), 3.31–3.40 (m, 1 H), 3.76–3.98 (m, 4 H), 5.84 (br d, $J = 5.58$ Hz, 1 H), 7.11 (d, $J = 8.42$ Hz, 2 H), 7.23 (d, $J = 8.46$ Hz, 2 H), 7.51 (br s, 1 H). ^{13}C NMR (CDCl_3): δ 23.05, 34.18, 46.76 (br), 50.67, 51.00, 63.05 (double peak), 128.15, 129.75, 131.25, 140.09, 172.01. Anal. Calcd for $\text{C}_{14}\text{H}_{20}\text{BClN}_2\text{O}_3$: C, 54.14; H, 6.49; B, 3.48. Found: C, 54.45; H, 6.42; B, 3.45.

D-Series. The inhibitors **D-1a–e** were prepared by the same methods as described above for the L-series. For each target and inhibitor, the IR and ^1H and ^{13}C NMR spectra were identical. Their other properties were as follows.

[(1*S*)-1-Acetamidoethyl]boronic Acid (D-1a). (–)-Pinanediol methylboronate (**ent-3a**; 41%), bp 60–65 °C (3 mmHg), $[\alpha]_D^{23} = -37.2$ (c 3.12 CHCl_3) (lit.^{18c} bp 85–87 °C (5 mmHg), $[\alpha]_D^{23,46} = -45.2$ (c 3.10 CHCl_3)). (–)-Pinanediol [(1*S*)-1-chloroethyl]boronate (**ent-4a**; 76%), bp 58–60 °C (0.1 mmHg), $[\alpha]_D^{23} = -32.9$ (c 2.06, toluene) (lit.^{18c} bp 80–82 °C (0.2 mmHg)). (–)-Pinanediol [(1*S*)-1-acetamidoethyl]boronate (**ent-5a**; 68%), mp 197–198 °C, $[\alpha]_D^{23} = -21.24$ (c 1.13, CHCl_3). [(1*S*)-1-Acetamidoethyl]boronic acid (**D-1a**; 89%), mp 185–188 °C, $[\alpha]_D^{23} = +81.3$ (c 0.47, H_2O). The HRMS was not obtainable so **D-1a** was further characterized as diethanolamine [(1*S*)-1-acetami-

doethyl]boronate (**D-6a**; 55%), mp 170–173 °C, $[\alpha]_D^{23} = +23.0$ (c 0.95, CH_2Cl_2). HRMS: calcd for $\text{C}_8\text{H}_{17}\text{BN}_2\text{O}_3$ 200.1332, found 200.1326.

[(1*S*)-1-Acetamido-2-phenylethyl]boronic Acid (D-1b). (–)-Pinanediol (phenylmethyl)boronate (**ent-3b**; 47%), bp 110–112 °C (0.2 mmHg), $[\alpha]_D^{23} = -30.6$ (c 6.30, toluene) (lit.^{17a} bp 110–112 °C (0.2 mmHg), $[\alpha]_D^{23} = -30.6$ (c 6.30 toluene)). (–)-Pinanediol [(1*R*)-1-chloro-2-phenylethyl]boronate (**ent-4b**; 89%), mp 46–47 °C, $[\alpha]_D^{23} = -24.8$ (c 2.25, toluene). (–)-Pinanediol [(1*S*)-1-acetamido-2-phenylethyl]boronate (**ent-5b**; 82%), mp 191–192 °C, $[\alpha]_D^{23} = +82.0$ (c 4.85, CHCl_3) (lit.^{17a} $[\alpha]_D^{23} = +82.1$ (c 4.00, CHCl_3)). [(1*S*)-1-Acetamido-2-phenylethyl]boronic acid (**D-1b**; 77%), mp 146–148 °C, $[\alpha]_D^{23} = +184.8$ (c 1.28, H_2O) (lit.^{15b} $[\alpha]_D^{23}$ as anhydride = +195.0 (c 0.70, H_2O)). HRMS: calcd for $\text{C}_{30}\text{H}_{36}\text{B}_3\text{N}_3\text{O}_6$ 567.2883, found 567.2899. Diethanolamine [(1*S*)-1-acetamido-2-phenylethyl]boronate (**D-6b**; 48%), mp 179–180 °C, $[\alpha]_D^{23} = +32.8$ (c 1.05, CH_2Cl_2). HRMS: calcd for $\text{C}_{14}\text{H}_{21}\text{BN}_2\text{O}_3$ 276.1645, found 276.1659.

[(1*S*)-1-Acetamido-2-(1-fluorophenyl)ethyl]boronic Acid (D-1c). (–)-Pinanediol [(4-fluorophenyl)methyl]boronate (**ent-3c**; 40%), bp 120–122 °C (0.35 mmHg), $[\alpha]_D^{23} = -29.06$ (c 6.04, toluene). (–)-Pinanediol [(1*R*)-1-chloro-2-(4-fluorophenyl)ethyl]boronate (**ent-4c**; 81%), mp 63–64 °C, $[\alpha]_D^{23} = -25.15$ (c 2.29, toluene). (–)-Pinanediol [(1*S*)-1-acetamido-2-(4-fluorophenyl)ethyl]boronate (**ent-5c**; 79%), mp 139–140 °C, $[\alpha]_D^{23} = +68.5$ (c 4.70, CHCl_3). [(1*S*)-1-Acetamido-2-(1-fluorophenyl)ethyl]boronic acid (**D-1c**; 66%), mp 132–135 °C, $[\alpha]_D^{23} = +156.0$ (c 0.72, H_2O). HRMS: calcd for $\text{C}_{30}\text{H}_{33}\text{B}_3\text{F}_3\text{N}_3\text{O}_6$ 621.2601, found 621.2589. Diethanolamine [(1*S*)-1-acetamido-2-(4-fluorophenyl)ethyl]boronate (**D-6c**; 62%), mp 197–200 °C, $[\alpha]_D^{23} = +30.3$ (c 0.74, CH_2Cl_2). HRMS: calcd for $\text{C}_{14}\text{H}_{20}\text{BFN}_2\text{O}_3$ 294.1551, found 294.1548.

[(1*S*)-1-Acetamido-2-(1-chlororophenyl)ethyl]boronic Acid (D-1d). (–)-Pinanediol [(4-chlorophenyl)methyl]boronate (**ent-3d**; 38%), mp 59–60 °C (Et_2O /hexanes), $[\alpha]_D^{23} = -26.3$ (c 6.00, toluene). (–)-Pinanediol [(1*S*)-1-chloro-2-(4-chlorophenyl)ethyl]boronate (**ent-4d**; 91%), mp 92 °C, $[\alpha]_D^{23} = -24.9$ (c 2.03, toluene). (–)-Pinanediol [(1*S*)-1-acetamido-2-(4-chlorophenyl)ethyl]boronate (**ent-5d**; 81%), mp 152–153 °C, $[\alpha]_D^{23} = +79.1$ (c 5.15, CHCl_3). [(1*S*)-1-Acetamido-2-(1-chlorophenyl)ethyl]boronic acid (**D-1d**; 79%), mp 138–141 °C, $[\alpha]_D^{23} = +156.0$ (c 0.72, H_2O). Anal. Calcd for $\text{C}_{10}\text{H}_{13}\text{BClNO}_3$: C, 49.74; H, 5.43; B, 4.48; N, 5.80. Found: C, 49.78; H, 5.11; B, 4.29; N, 5.98. Diethanolamine [(1*S*)-1-acetamido-2-(4-chlorophenyl)ethyl]boronate (**D-6d**; 54%), mp 216–218 °C, $[\alpha]_D^{23} = +25.0$ (c 0.60, CH_2Cl_2). HRMS: calcd for $\text{C}_{14}\text{H}_{20}\text{BClN}_2\text{O}_3$ 310.1256, found 310.1258.

[(1*S*)-1-Acetamido-2-(1-naphthyl)ethyl]boronic Acid (D-1e). (–)-Pinanediol (1-naphthylmethyl)boronate (**ent-3e**; 41%), bp 160–165 °C (0.2 mmHg), $[\alpha]_D^{23} = -24.2$ (c 6.78, toluene). (–)-Pinanediol [(1*R*)-1-chloro-2-(1-naphthyl)ethyl]boronate (**ent-4e**; 81%), obtained as an oil after chromatography on silica gel, $[\alpha]_D^{23} = -22.5$ (c 2.56, toluene). (–)-Pinanediol [(1*S*)-1-acetamido-2-(1-naphthylethyl)boronate (**ent-5e**; 68%), mp 238–240 °C, $[\alpha]_D^{23} = +55.7$ (c 2.97, CHCl_3). [(1*S*)-1-Acetamido-2-(1-naphthyl)ethyl]boronic acid (**D-1e**; 47%), mp 168–172 °C, $[\alpha]_D^{23} = +141.4$ (c 1.35, CH_3OH). HRMS: calcd for $\text{C}_{22}\text{H}_{24}\text{B}_3\text{N}_3\text{O}_6$ 717.3353, found 717.3398. Diethanolamine [(1*S*)-1-acetamido-2-(1-naphthylethyl)boronate (**D-6e**; 40%), mp 242–245 °C dec, $[\alpha]_D^{23} = +130.6$ (c 0.61, CH_2Cl_2). HRMS: calcd for $[\text{M} + \text{H}]^+ \text{C}_{18}\text{H}_{24}\text{BN}_2\text{O}_3$ 327.1883, found 327.1867.

Computational Methods. System Setup. The reference structures used were those of McPhalen and James^{4a} for the subtilisin Carlsberg–eglin C complex and of Tsukada and Blow^{5b} for α -chymotrypsin, both available from the Protein Data Bank²⁸ at Brookhaven National Laboratory.²⁹ The setup was done with Insight II, version 2.2.0 (Biosym Technologies, Inc., San Diego, CA). To create initial coordinates for the minimization of SC, the inhibitor (eglin C) and the three calcium ions were removed. In the case of CT, the dimeric structure of the enzyme was split into its individual, independent monomers. Only one

(28) For the subtilisin Carlsberg entry 2SEC, 1.8 Å resolution; for α -chymotrypsin entry 4CHA, 1.68 Å resolution.

(29) (a) Bernstein, F. C.; Koetzle, T. F.; Williams, J. B.; Meyer, E. F., Jr.; Brice, M. D.; Rodgers, J. R.; Kennard, O.; Shimanouchi, T.; Tasumi, M. *J. Mol. Biol.* **1977**, *112*, 535. (b) Abola, E. E.; Bernstein, F. C.; Bryant, S. H.; Koetzle, T. F.; Weng, J. In *Crystallographic Databases – Information Content, Software Systems, Scientific Applications*; Allen, F. H., Bergerhoff, G., Sievers, R., Eds.; Data Commission of the International Union of Crystallography: Bonn/Cambridge/Chester, 1987; p 107.

of the monomers was used to create the initial coordinates for the enzyme. Residues Gly12 and Leu13, missing due to poor X-ray resolution, were added using Insight. Hydrogen atoms were added at the pH (7.8) used for the kinetic measurements. This protonated all Lys, Arg, and His residues and the N-terminus and deprotonated the acids Glu and Asp and the C-terminus on both enzymes. In the calculations of the boronic acid–enzyme complexes, a tetrahedral carbon atom was used to mimic the boron atom since, as yet, no force field parameters have been reported for boron. This approximation was considered acceptable since only energy differences resulting from changes remote from boron were being explored. To set up the initial structure for the energy minimization, the boron-equivalent carbon was covalently bound to the oxygen of the hydroxyl group of the active site Ser221 of SC. The X-ray structures of 2-phenethylboronic acid bound to subtilisin BPN³⁰ and α -lytic protease (mutant with Met192 replaced by Ala) complexed with (methoxysuccinyl-Ala-Ala-Pro-phenylalanyl)boronic acid³¹ were used as the models to guide dockings of the acetamido acids of Table 1 into the active site of SC. The two hydroxy groups attached to the boron were oriented such that one pointed to the oxyanion hole, formed by NH₂ of Asp155 and the backbone NH of Ser221, and the other to His64, which becomes positively charged after the addition of the proton from Ser221. The aromatic residue of each inhibitor was positioned in the S₁-pocket (defined by Ser125–Ala129, Ala152–Ser156, and Ile165–Tyr167) in a manner that avoided all bad van der Waals interactions. To determine the position of the acetamido group within the S₂-pocket, the structure of SC was superimposed on that of the α -lytic protease complexed with (methoxysuccinyl-Ala-Ala-Pro-phenylalanyl)boronic acid. This positioned the acetamido within S₂ such that a hydrogen bond was created between the amide hydrogen of the inhibitor and the carbonyl oxygen of Ser125.³²

A similar docking procedure was used for CT, with the reference structure used for docking being that of CT complexed with (2-phenylethyl)boronic acid.^{5e} One of the hydroxyls of the boronic acid was directed to the oxyanion hole, formed by the backbone NH's of Gly193 and Ser195, and the other to the positively charged His57 of the catalytic triad. The aromatic ring of each inhibitor was positioned in the S₁-pocket (defined by Val213–Thr219, Ser190–Asp194, Ser189, and Gly226) and the acetamido group within the S₂-site such that a hydrogen bond formed between the amide hydrogen of the inhibitor and the carbonyl oxygen of Ser214.

Charges on the active site serine and the enzyme-bound boronic acid for both complexes were generated by single-point MNDO³³/ESP³⁴ calculations (MOPAC 93³⁵) and scaled to fit those of the CVFF (consistent valence force field) library. The overall negative charge of -1 was mostly on, and distributed between, the oxygen atoms bound to boron. The boron atom itself was assigned a charge of -0.01 . This model system was solvated in a rectangular box ($49 \times 47 \times 49 \text{ \AA}^3$) of water molecules. The total number of water molecules in this system was 2318. The overall charge of the enzyme–inhibitor complex resulting from this setup was -1 .

Energy Minimization. The simulations were performed with the Discover program, version 2.9.0 (Biosym Technologies, Inc., San Diego, CA) on a Silicon Graphics 240 GTX computer, using the CVFF.³⁶ A nonbonded cutoff of 10 \AA with a switching function between 7.5 and 9 \AA was used. The nonbonded pair list was updated every 20 cycles, and a dielectric constant of 1 was used in all calculations. The energy of the system was minimized with respect to all 3N Cartesian coordinates until the maximum derivative of $0.1 \text{ kcal mol}^{-1} \text{ \AA}^{-1}$ was reached. The resulting structure was used as the starting point for the

molecular dynamics calculations. During the molecular dynamics (MD) simulations, the whole enzyme, with the exception of a 12 \AA radius region around Ser221, was kept fixed, as were water atoms more than 15 \AA away from Ser221. The molecular dynamics simulations were performed for an initial equilibrium period of 10 ps at 400 K, and then continued for 20 ps at 400 K, with a time step of 10 fs. The 400 K temperature of the MD simulations ensured that there was no trapping in local minima. The molecular dynamics trajectories were animated using the Analysis module of Insight, and a set of the structures was selected visually. We assumed that the aromatic ring of all inhibitors would bind into the S₁-pocket of both enzymes. In cases where the aromatic ring of the inhibitor left the pocket during the molecular dynamics simulations (for example, as it did for L- and D-**1e** in orientation (a) of Figure 1 for SC), the structures were discarded. Each selected structure was cooled to 300 K by initializing the molecular dynamics at 300 K and then minimizing, first using steepest descents until the maximum derivative was less than 5.0 kcal/\AA , and then using a conjugate gradient, until the maximum derivative was less than 0.1 kcal/\AA . The results are summarized in Figures 2 and 3. For the strong hydrogen bonds, the calculated heteroatom distances (\AA) were as follows.

Subtilisin Carlsberg. For L-(R)-**1e**: boron O(1) to side chain N of Asn155, 3.09 ± 0.33 ; to backbone N of Ser221, 3.18 ± 0.28 ; boron O(2) to N ϵ of His64, 2.96 ± 0.31 ; acetamido N to CO of Ser125, 3.01 ± 0.33 . For D-(S)-**1e**: boron O(1) to side chain N of Asn155, 3.33 ± 0.46 ; to backbone N of Ser221, 3.31 ± 0.50 ; boron O(2) to N ϵ of His64, 3.86 ± 0.66 .

(α)-Chymotrypsin. For D-(S)-**1e**: boron O(1) to backbone N of Ser195, 3.21 ± 0.62 ; to backbone N of Gly193, 3.61 ± 0.56 ; acetamido CO to N ϵ of His57, 3.05 ± 0.31 . For L-(R)-**1e**: boron O(1) to backbone N of Ser195, 3.12 ± 0.46 ; to backbone N of Gly193, 3.03 ± 0.37 .

Kinetic Measurements. The enzyme kinetics were performed under steady-state conditions at $25 \text{ }^\circ\text{C}$ using a pH-stat.^{2d} In order to prevent any oxidation of the boronic acids, all measurements were done under argon using water degassed with argon at reflux. For SC, the reference substrate was *N*-*p*-tosyl-L-arginine methyl ester (TAME) and the following basic procedure was employed. After adjusting the pH to 7.0 with 0.2 M NaOH, 0.01–1.00 mL of the inhibitor solution (1.0×10^{-5} to $5.0 \times 10^{-1} \text{ M}$ in water) was added to the reaction mixture containing 0.187 M TAME solution (aliquots of 0.4, 0.6, 0.8, 1.0, 2.0, 4.0, and 8.0 mL), 1 M KCl solution (1 mL), and water to bring the final volume to 10 mL and to give final concentrations of 7.5×10^{-3} to $1.5 \times 10^{-1} \text{ M}$ substrate and 10^{-7} to $5.0 \times 10^{-2} \text{ M}$ inhibitor. After equilibration for 3 min, the pH was adjusted to 7.8 with 0.2 M NaOH and the reaction initiated by addition of 50 μL of SC stock solution ($4.0 \times 10^{-5} \text{ M}$ in 0.01 M phosphate buffer, pH 7.8). The rate of uptake of 0.2 M NaOH was recorded directly into a PC.

The kinetics data for CT were determined similarly, using the following stock solutions: $3.8 \times 10^{-3} \text{ M}$ *N*-acetyl-L-tyrosine ethyl ester (NATEE) as a substrate (aliquots 0.4, 0.6, 0.8, 1.0, 2.0, 4.0, 8.0 mL), 1 M KCl solution (1 mL), inhibitor (1.0×10^{-5} to $5.0 \times 10^{-1} \text{ M}$ in water), and enzyme ($4.0 \times 10^{-7} \text{ M}$ in 0.001 M HCl). The final concentration of substrate was 1.5×10^{-4} to $3.0 \times 10^{-3} \text{ M}$. After initiation of the reaction by addition of 50 μL of CT stock solution, the rate of the reaction was monitored by uptake of 0.02 M NaOH.

K_I values were determined using the Grafit program (Erithacus Software Ltd., U.K.). All kinetic runs were performed in duplicate at two different concentrations of boronic acids. The results are recorded in Table 1.

Acknowledgment. Support from the Natural Sciences and Engineering Research Council of Canada is gratefully acknowledged.

Supporting Information Available: Figures showing ¹H and ¹³C NMR spectra for L-**1b,d,e**, L-**6b**, D-**1b,c,e**, and D-**6a–e** (24 pages). This material is contained in libraries on microfiche, immediately follows this article in the microfilm version of the journal, can be ordered from the ACS, and can be downloaded from the Internet; see any current masthead page for ordering information and Internet access instructions.

(30) Matthews, D. A.; Alden, R. A.; Birktoft, J. J.; Freer, S. T.; Kraut, J. *J. Biol. Chem.* **1975**, *250*, 1720.

(31) Bone, R.; Silen, J. L.; Agard, D. A. Entry 1P08 in the Brookhaven Protein Database, 2.25 \AA resolution.

(32) Robertus, J. D.; Alden, R. A.; Birktoft, J. J.; Kraut, J. J.; Powers, J. C.; Wilcox, P. E. *Biochemistry* **1972**, *11*, 2439.

(33) (a) Dewar, M. J. S.; Theil, W. *J. Am. Chem. Soc.* **1977**, *99*, 4899. (b) Martin, J. M. L.; Francois, J. P.; Gijbels, R. *J. Comput. Chem.* **1991**, *12*, 52.

(34) Besler, B. H.; Merz, K. M. Jr.; Kollman, P. A. *J. Comput. Chem.* **1990**, *11*, 431.

(35) MOPAC 93.00 Manual: J. J. P. Stewart, Fujitsu Limited, Tokyo, Japan, 1993.

(36) Hagler, A. T.; Osguthorpe, D. J.; Dauber-Osguthorpe, P.; Hempel, J. C. *Science* **1985**, *227*, 1309.